

Mathematical Model to Predict the Affinity Between Aggregate/Bitumen

P. Caputo¹, G.A. Ranieri¹, D. Miriello², A. Bloise², A.A. Abe¹, B. Teltayev³, C. Oliviero Rossi^{1*}

¹Department of Chemistry and Chemical Technologies, University of Calabria,
Via P. Bucci, Cubo 14/D, 87036 Arcavacata di Rende (CS), Italy

²Department of Biology, Ecology and Earth Sciences, University of Calabria, 87036 Arcavacata di Rende, CS, Italy

³Kazakhstan Highway Research Institute, 2A Nurpeisova Str., Almaty, Kazakhstan

Article info

Received:

18 January 2020

Received in revised form:

26 March 2020

Accepted:

15 May 2020

Keywords:

Bitumen/aggregate affinity
Rolling Bottle Test
Boiling Test
X-ray powder diffraction

Abstract

The stones used for the construction of road surfaces have a complex mineralogical and hence chemical composition. They are made up of several types of minerals put together. This generates a significant difference in adhesion with the bituminous binder. The aim of this study is to create a mathematical model able to predict the adhesion between bitumen and stone on the basis of contact angle measurements made on different pure minerals. The mathematical model used was developed keeping in mind the exponential bond that the minerals have with the corresponding bond angle. This model also confirmed the established fact that the lower the value of Δ , the better the adhesion between the bitumen and the aggregate.

1. Introduction

Road pavements are made up of over 93% stones and less than 7% of bitumen which works as a binder. Bitumen is a soft multicomponent material that is derived from petroleum industry processes. For this reason, its chemical composition is complex and different additives can be used to improve its properties [1–13]. To reduce atmospheric emissions and costs during the laying of bitumen on the roads, some additives can be used able to make the conglomerates more workable at lower temperatures [14, 18].

Depending on the chemical nature of the stones and bitumen, there can be a greater or lesser affinity between the two and this significantly affects the road life span.

Before of the processing of asphalt concrete, adhesion tests are generally carried out (Boiling Test, Rolling Bottle Test, Contact Angle, etc.) to check the compatibility between the aggregate and

bitumen and possibly [19–23], if the latter is insufficient, intervene with additives called adhesion activators [24–30].

Empirical tests such as the Boiling Test deliver a fast but very indicative evaluation of the affinity between aggregate and bitumen. Contact angle measurements actually facilitate having more accurate data, even if they involve using more sophisticated and expensive equipment and require higher lead times.

The goal of this study is to create a purely theoretical model that allows you to predict the adhesion between stone and bitumen, using the contact angle values recorded between the bitumen and each mineral that makes up the aggregate. For this purpose, contact angle measurements were made between the binder and several pure minerals, in order to create a database of some sort containing the information necessary for the development of the theoretical model. To evaluate the effectiveness and validity of the model, three stones were tested and contact angle measurements in conjunction with further Boiling Test measurements were carried out on them.

*Corresponding author.

E-mail: cesare.oliviero@unical.it

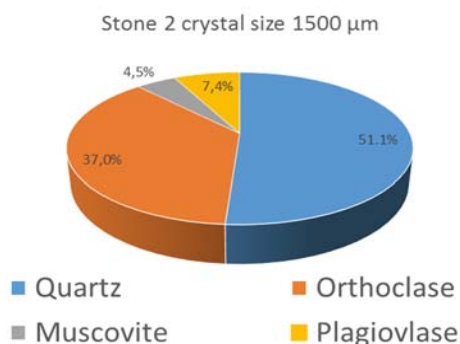
Both the aggregates and the minerals were characterized by X-ray analysis. The samples differ only in the chemical nature of the stones and the minerals being that only one type of bitumen was used for all measurements.

2. Materials

2.1. Bitumen binder

In this study, a 50/70 bitumen was used which was kindly supplied by Loprete Costruzioni Stradali. The bitumen was produced in Italy, while the crude oil was from Saudi Arabia. Reported below are some of the physical properties of the bitumen:

- Penetration Grade (59 ± 1) 0.1 mm in according to ASTM standard D946;
- Softening point R&B (51.7 ± 1) °C in according to ASTM Standard D36;
- Asphaltene content (27.1 ± 0.1) w/w % by Modified Conventional Method [31].



2.2. Stones

Three stones were analysed in this study. Figures 1 and 2 show the XRD analysis results for the mineralogical composition and the crystal sizes for each sample, while information about the characteristics of the 15 minerals analysed is given in Table 1 [32]. These stones were kindly supplied by Cosentina Marmi (Italy).

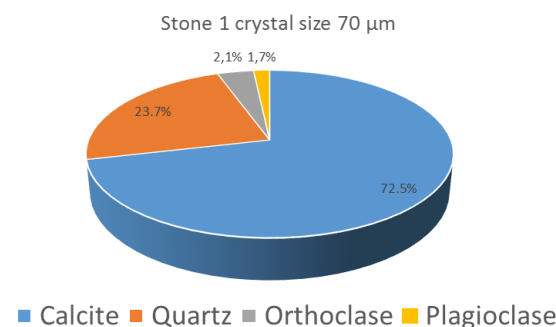


Fig.1. XRD analysis, the mineral composition (fine grain) Calcarenite.

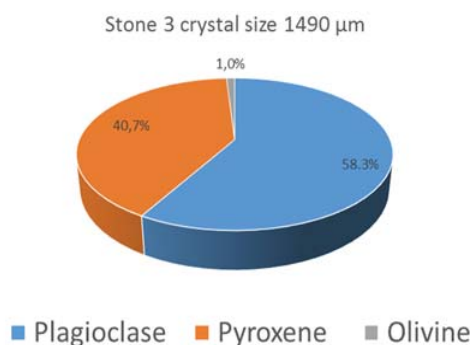


Fig. 2. XRD analysis, the mineral composition (medium grain) of the used stones: (a) – Granite and (b) – Basalt.

3. Methods

3.1. Contact Angle Measurements (CAM)

All stones were cut to obtain smooth surfaces with adept precision using the MT100 Remet cutting machine, with a diamond blade (300 mm) Wendt Boart. The stones were then polished with a fine polishing cloth ALKASEL (diameter gran size 1 μm), washed with water and dried at room temperature for 24 h. Subsequently, using a needle, three drops of hot bitumen (at 150 °C) were dropped on the stones of each sample (at room temperature).

When preparing the samples for contact angle measurement, the drop size of the bitumen on the stone is very important to get correct results [33–35].

The contact angle measurement was made through the following steps:

1. The samples were kept at 25 °C for 10 min.
2. The samples were kept for 10 min at 25 to 30 °C higher than the R&B of the bitumen, and then cooled to room temperature for 10 min.
3. The samples were kept for 2 h at a temperature of 5 °C less than the R&B of the bitumen, dried and cooled to room temperature for 10 min.

For each step, the measurements were made at room temperature. The adhesion was evaluated using the contact angle obtained in step 2 and 3 using Eq. 1 as follows:

$$\Delta = \text{Contact Angle STEP3} - \text{Contact Angle STEP2} \quad (\text{Eq.1})$$

Table 1
Characteristics and chemical composition of the minerals

Mineral	Cleavage	Hardness (Mohs)	Density gm/cc	Photoelectric barns/electron	Fermion Index	Boson Index	Chemical Composition (%)
GARNET	No	7	3.5	1.59	0.02	0.98	29.99 MgO/44.71 SiO ₂ /25.3 Al ₂ O ₃
PYROXENE	Yes	6	3.19	1.61	0.03	0.97	40.15 MgO/59.85 SiO ₂
GYPSUM	Yes	2	2.36	3.97	0.0019	0.99	32.57 CaO/20.93 H ₂ O/46.5 SO ₃
ANALCIME	No	5.5	2.27	1.52	0.01	0.99	54.58 SiO ₂ /8.18 H ₂ O/23.16 Al ₂ O ₃ /14.08 Na ₂ O
ORTOCLASE	No	6.	2.6	2.85	0.01	0.99	64.76 SiO ₂ /16.92 K ₂ O/18.32 Al ₂ O ₃
DOLOMITE	Yes	4	2.84	3.13	0.01	0.99	30.40 CaO/21.90 MgO/47.70 CO ₂
PYRITE	No	6.5	4.84	16.89	0.01	0.99	46.55 Fe/53.45 S
MUSCOVITE	Yes	2	2.8	2.39	0.01	0.99	45.21 SiO ₂ /4.62 H ₂ O/11.81 K ₂ O/38.36 Al ₂ O ₃
TALC	Yes	1	2.75	1.57	0.03	0.97	31.88 MgO/63.37 SiO ₂ /4.75 H ₂ O
BIOTITE	Yes	3	3.09	4.04	0.02	0.98	23.24 MgO/41.58 SiO ₂ /4.27 H ₂ O/10.86 K ₂ O/11.76 Al ₂ O ₃ /8.29 FeO
QUARTZ	No	7	2.65	1.8	0.02	0.98	100 SiO ₂
CALCITE	Yes	3	2.71	5.06	0.002	0.99	56.03 CaO/43.97 CO ₂
TOURMALINE	No	7	2.99	1.42	0.02	0.98	12.61 MgO/37.60 SiO ₂ /3.76 H ₂ O/31.90 Al ₂ O ₃ /3.23 Na ₂ O/10.90 B ₂ O ₃
PLAGIOCLASE	Yes	7	2.62	1.75	0.01	0.99	67.39 SiO ₂ /20.35 Al ₂ O ₃ /1.07 CaO/11.19 Na ₂ O
OLIVINE	No	7	3.27	1.53	0.04	0.96	57.29 MgO/42.71 SiO ₂

Consequently, the contact angle measurements established that the lower the value of Δ the greater the affinity/adhesion between the bitumen and the mineral. More details can be found in reference [36].

3.2. Boiling test

The boiling test procedure used in this study was performed according to ASTM D3625 [37]. All details can be found in reference [25].

3.3. Petrographic characterization

To characterize the petrographic qualities, X-ray powder diffraction XRPD patterns were used. The XRPD patterns were obtained by a Bruker D8 Advance (Bruker, Billerica, MA, USA) X-ray diffractometer with the use of CuK α radiation, monochromated with a graphite sample at 40 kV and 40 mA. Scans were conducted in the range of 3°–66° (2 θ), with a step interval of 0.02° and a step-counting time of 3 s. The mineral phases of the stones were identified using the EVA software (DIFFRACplus

EVA). The peaks were then compared with the 2005 PDF2 reference patterns; this software compares the experimental peaks with the 2005 PDF2 reference patterns. An estimate of the mineralogical phases and amorphous substances present in the samples was obtained by Rietveld refinements [38–40] carried out using TOPAS software V.4.2 (Bruker, Karlsruhe, Germany).

4. Results and discussion

A stone can be considered as an entirety of different minerals [41], each of which has its own chemical nature. Consequently, each of them has a different interaction with bitumen. The chemical composition of the bitumen is another important factor that affects adhesion, but in this study, since only one type of binder is used, this parameter is to be considered constant for all samples. Another determining parameter for adhesion is the size of the individual crystals that make up the stone [42]. In fact, the presence of large crystals or crystals with sizes similar to the bitumen drops used, make

Table 2
Contact Angle values of some pure minerals with the reference bitumen

Mineral	Step 1	Step 2	Step 3	Δ (°)
GARNET	120.7	72.7	74.3	1.6
PYROXENE	120.6	80.8	82.8	2.0
GYPSUM	122.9	52.6	66.8	14.2
ANALCIME	118.7	81.6	100.0	18.4
ORTHOCLASE	126.8	76.6	77.4	0.8
DOLOMITE	128.5	51.7	56.4	4.7
PYRITE	125.5	42.8	46.1	3.3
MUSCOVITE	103.3	38.1	118.1	80.0
TALC	113.4	54.7	111.7	57.0
BIOTITE	98.9	27.9	74.1	46.2
QUARTZ	116.0	30.9	41.9	11.0
CALCITE	126.6	54.8	60.4	5.6
TOURMALINE	117.2	52.0	59.0	7.0
PLAGIOCLASE	109.5	72.9	79.5	6.6
OLIVINE	123.2	62.3	108.3	46.0

the contact angle measurements more uncertain than for samples with small grain or crystals. This is most likely due to the fact that the surrounding minerals often have a very different affinity for bitumen and if the grain is large, areas are created on the surface of the aggregate. These areas of space account for a huge difference in adhesion which can lead to a worsening in the magnitude of the contact angle, a less evident problem when the grain is fine, since the surface is more homogeneous. This problem was alleviated by choosing fine or medium grain stones for this study and by performing an adequate number of measurements in order to obtain reliable mediated values.

Table 2 shows the results obtained through contact angle measurements made with our bitumen of reference on 15 different types of pure minerals [43]. Boiling tests could not be carried out on these minerals because the extremely small quantities and dimensions of the pure mineral samples were not sufficient and suitable for carrying out a test in accordance with ASTM D3625 regulations.

From the results obtained, it is clear that the minerals that have better adhesion with the bitumen used are: Orthoclase, Garnet, Pyroxene, Pyrite and Dolomite. The latter in fact has a Δ very close to zero, this indicates that the angle was not significantly influenced by the action of water and temperature in step 3. To confirm this, the contact angle values recorded in the last step was the lowest obtained.

On the other hand, Biotite, Talc, Olivine and Muscovite have a poor affinity with bitumen.

4.1. Mathematical Model

Assuming we can carry out Boiling Tests on pure minerals (as already stated to be impossible), we can easily hypothesize that the percentage of coating achieved on the individual minerals exploits the additive property given that the mineral mixtures form the stones. Keeping in mind the exponential bond that these have with the corresponding contact angle, we can assume the following empirical formula:

$$\text{Theoretical Contact Angle (TCA)} = \ln \left[\frac{\sum_{i=1}^N f_i e^{\Delta_i}}{\sum_{i=1}^N f_i} \right] \quad (\text{Eq. 2})$$

where f_i and Δ_i are respectively the percentage and the contact angle of the i^{th} mineral present in the stone, and TCA the resulting contact angle of the analysed stone.

The validity of the model is tested on 3 types of stones with 3 different mineralogical compositions characterized by X-ray, with different grain sizes ranging from 70 to 1500 μm (see mineralogical composition shown in Figs. 1 and 2).

Table 3 shows values obtained by means of experimental contact angle measurements carried out directly on the stones. These values are called Measured Contact Angle (MCA) while those ob-

Table 3
MCA, CBT, TCA, TBT and MBT calculated/measured for the analysed stones MBT

Stones mean crystal size	Minerals	MCA/CBT Stones	TCA/TBT Stones	MBT Stones
Stone 1 (Calcarenite) 70 μm	Calcite 72.5% $\Delta = 5.6^\circ$	10° = 57%	14° = 49%	65%
	Quartz 23.7% $\Delta = 11^\circ$			
	Orthoclase 2.1% $\Delta = 0.8^\circ$			
	Plagioclase 1.7% $\Delta = 6.6^\circ$			
Stone 2 (Granite) 1500 μm	Quartz 51.1% $\Delta = 11^\circ$	79° = 4.1%	82° = 3.7%	5%
	Orthoclase 37.0% $\Delta = 0.8^\circ$			
	Muscovite 4.5% $\Delta = 80^\circ$			
	Plagioclase 7.4% $\Delta = 6.6^\circ$			
Stone 3 (Basalt) 1490 μm	Plagioclase 58.3% $\Delta = 6.6$	35° = 22%	46° = 23%	15%
	Pyroxene 40.7% $\Delta = 2.0^\circ$			
	Olivine 1% $\Delta = 46^\circ$			

tained according to the theoretical model for predicting the adhesion in Eq. 2 are called Theoretical Contact Angle (TCA) in addition to the results carried out on the same stones.

Having calculated the TCA, it was also possible to derive the percentage of theoretical coating of the Boiling Test (TBT) using the formula proposed in the article [34], whose parameters were obtained from samples by the same methodology. In the same way it was possible to obtain CBT (calculated boiling test) for stones from the MCA.

$$TBT = 83,4e^{-0.038 TCA}; \quad (\text{Eq. 3.1})$$

$$CBT = 83,4e^{-0.038 MCA}; \quad (\text{Eq. 3.2})$$

In Eq. 2 the constants of Eqs. 3.1 and 3.2 are both canceled, because the inverse function of the same exponential function is applied.

Boiling Test Measures were also carried out directly on the examined stones (MBT) to compare them directly with those obtained through Eqs. 2 and 3 (see Table 3).

In summary, the differences in absolute value between MCA/TCA and MBT/TBT for every single stone are as follows.

In Table 4, the average between MBT and CBT divided by TBT was calculated. We observe that the values are in close range of each other: this result confirms that the mathematical model is trustworthy. In particular, it shows the differences in contact angle and boiling test between the measured values obtained in our experiments, the calculated values and the theoretical values obtained by using the suggested mathematical model. Although all three stones had values that are close to

the theoretical values, stone 2 has the lowest difference in values between the theoretical and practical phenomena hence it is the most suitable among the samples.

These results demonstrate how possible it is to predict using Eq. 2, the adhesion between stone and binder, knowing its mineralogical composition and the affinity between each individual mineral and the bitumen used. In Eq. 2, the contact angles become an exponential function, consequently, the mineral that has greater contact angle (Δ) is dominant with respect to the other minerals even if present in low percentages in the mineralogical composition of the stone.

One of the main limitations of the contact angle technique is that it cannot be used for stones formed from coarse-grained crystals ($> 2000 \mu\text{m}$). In this study, no experiments were conducted with stones formed from coarse-grained crystals given that the experimental measurements are highly dependent on the size of the crystals that make up the analysed stone. Even though the measurements made on each individual mineral are independent of this parameter, we can assume that the TCA value calculated for coarse-grained stones may be closer to the real affinity between aggregate and bitumen than any MCA carried out directly on the stone.

Table 4
MCA-TCA, MBT-TBT, (MBT+CBT)/2 -TBT value are reported

Sample	MCA-TCA (°)	MBT-TBT (%)	(MBT + CBT) / 2 -TBT (%)
Stone 1	4.0	16	12
Stone 2	3.0	1.3	0.9
Stone 3	11	8.0	4.5

5. Conclusion

By determining the adhesion between pure minerals and a specific bitumen while knowing the mineralogical composition of aggregate, it is possible to predict the affinity of the latter with bitumen using the model of Eq. 2. This work gives a theoretical indication of adhesion but is complicated to apply it practically.

In order to use Eq. 2, it is necessary to have the affinity data between the minerals and bitumen used and this involves conducting contact angle measurements with pure minerals for each type of bitumen you want to use. Furthermore, to obtain accurate results, once the bitumen has been selected, the surfaces of the minerals must be perfectly smooth. Contact angle measurements from different observation points can then be made around the bitumen drop and then the resulting values are averaged. The experimental indications reported in reference [36] should be followed in order to obtain accurate data. It is important to note that as long as the mineralogical composition of the stone comprises a mineral with a Δ significantly greater than the other minerals even if it is present in small percentages, the value of the latter will be greatly influenced. For example, in stone 3, Olivina that has a Δ of 46° is present with a mineralogical composition of 1%. The final contact angle (TCA) of the stone is 46° which is the same as the value of Δ regardless of the low percentage. This is justified by the fact that in Eq. 2, the contact angles are exponential functions. The practical disadvantage is that this technique requires special equipment, both to make the measurements and to prepare the samples while also requiring long processing times. All these lead to long durations and high costs which are unfavorable. However, once a database with used stones and bitumen has been created, it will be possible to foresee the adhesion simply by developing Eq. 2 without needing to carry out further measurements thus identifying the best stone/bitumen combination.

The main purpose of this work was to provide through the definition of Eq. 2, a mathematical confirmation of both the correlation between the Boiling Test and the contact angle as well as between the adhesion of the individual minerals and the respective stones.

In conclusion, from the results obtained, we can affirm that it is possible to predict the adhesion between a specific aggregate and a bitumen knowing its mineralogical composition and the adhesion behaviour of each individual mineral which makes

up the stone. In particular, as long as in the mineralogical composition of the stone, a mineral is present with a Δ much higher than the other stone minerals, the final value of the contact angle can be approximated to that of the pure mineral even if present in a low percentage.

References

- [1]. S. Rozeveld, E. Shin, A. Bhurke, L. France, L. Drzal, *Microsc. Res. Technol.* 38 (1997) 529–543. DOI: [10.1002/\(SICI\)1097-0029\(19970901\)38:5<529::AID-JEMT11>3.0.CO;2-O](https://doi.org/10.1002/(SICI)1097-0029(19970901)38:5<529::AID-JEMT11>3.0.CO;2-O)
- [2]. J.B. Król, K.J. Kowalski, L. Niczke, P. Radziszewski, *Constr. Build. Mat.* 114 (2016) 194–203. DOI: [10.1016/j.conbuildmat.2016.03.086](https://doi.org/10.1016/j.conbuildmat.2016.03.086)
- [3]. C. Oliviero Rossi, P. Caputo, S. Ashimova, A. Fabozzi, G. D'Errico, R. Angelico, *Appl. Sci.* 8 (2018) 1405. DOI: [10.3390/app8081405](https://doi.org/10.3390/app8081405)
- [4]. M. Porto, P. Caputo, V. Loise, S. Eskandarsefat, B. Teltayev, C. Oliviero Rossi, *Appl. Sci.* 9 (2019) 742. DOI: [10.3390/app9040742](https://doi.org/10.3390/app9040742)
- [5]. P. Caputo, M. Porto, V. Loise, B. Teltayev, C. Oliviero Rossi, *Eurasian Chem.-Technol. J.* 21 (2019) 235–239. DOI: [10.18321/ectj864](https://doi.org/10.18321/ectj864)
- [6]. M. Porto, P. Caputo, V. Loise, G. De Filipo, C. Oliviero Rossi, P. Calandra, *Appl. Sci.* 9 (2019) 5564. DOI: [10.3390/app9245564](https://doi.org/10.3390/app9245564)
- [7]. H. Jaroszek, *CHEMIK* 66 12 (2012) 1340-1345.
- [8]. C. Qian, W. Fan, F. Ren, X. Lv, B. Xing, *Constr. Build. Mat.* 227 10 (2019) 117094. DOI: [10.1016/j.conbuildmat.2019.117094](https://doi.org/10.1016/j.conbuildmat.2019.117094)
- [9]. S.-peng Wu, L. Pang, L.-tong Mo, Y.-chun Chen, G.-jun Zhu, *Constr. Build. Mat.* 23 (2009) 1005–1010. DOI: [10.1016/j.conbuildmat.2008.05.004](https://doi.org/10.1016/j.conbuildmat.2008.05.004)
- [10]. H. Zhang, J. Yu, S. Wu, *Constr. Build. Mat.* 27 (2012) 553–559. DOI: [10.1016/j.conbuildmat.2011.07.008](https://doi.org/10.1016/j.conbuildmat.2011.07.008)
- [11]. F.J. Navarro, P. Partal, F. Martinez-Boza, C. Gallegos, *Energ. Fuel.* 19 (2005) 1984–1990. DOI: [10.1021/ef049699a](https://doi.org/10.1021/ef049699a)
- [12]. J.S. Chen, C.C. Huang, P.Y. Chu, K.Y. Lin, *J. Mater. Sci.* 42 (2007) 9867–9876. DOI: [10.1007/s10853-007-1713-8](https://doi.org/10.1007/s10853-007-1713-8)
- [13]. J.-F. Su, J. Qiu, E. Schlangen, Y.-Y. Wang, *Constr. Build. Mat.* 74 (2015) 83–92. DOI: [10.1016/j.conbuildmat.2014.10.018](https://doi.org/10.1016/j.conbuildmat.2014.10.018)
- [14]. P. Caputo, G.A. Ranieri, N. Godbert, I. Aiello, A. Tagarelli, C. Oliviero Rossi, *Mediterranean Journal of Chemistry* 7 (2018) 259–266. DOI: [10.13171/mjc74181107-rossi](https://doi.org/10.13171/mjc74181107-rossi)
- [15]. M. Arabani, H. Roshani, G.H. Hamed, *J. Mater. Civil Eng.* 24 (2012) 889–897. DOI: [10.1061/\(ASCE\)MT.1943-5533.0000455](https://doi.org/10.1061/(ASCE)MT.1943-5533.0000455)

- [16]. G.C. Hurley, B.D. Prowell, Evaluation of Sasobit® for Use in Warm Mix Asphalt. National Center for Asphalt Technology, NCAT Report 05-06, 2005, 27 p.
- [17]. A. Stimilli, A. Virgili, F. Canestrari, *J. Clean. Prod.* 156 (2017) 911–922. DOI: [10.1016/j.jclepro.2017.03.235](https://doi.org/10.1016/j.jclepro.2017.03.235)
- [18]. S.D. Capitão, L.G. Picado-Santos, F. Martinho, *Constr. Build. Mater.* 36 (2012) 1016–1024. DOI: [10.1016/j.conbuildmat.2012.06.038](https://doi.org/10.1016/j.conbuildmat.2012.06.038)
- [19]. U. Bagampadde, U. Isacson, B.M. Kiggundu, *Road Mater. Pavement Design* 5 (2004) 7–43. DOI: [10.1080/14680629.2004.9689961](https://doi.org/10.1080/14680629.2004.9689961)
- [20]. J.G. Speight, *Asphalt Materials Science and Technology*, Butterworth-Heinemann, 2015. DOI: [10.1016/C2013-0-15469-4](https://doi.org/10.1016/C2013-0-15469-4)
- [21]. D. Little, D.H. Allen, A. Bhasin, *Modeling and Design of Flexible Pavements and Materials*, Springer International Publishing, 2018. DOI: [10.1007/978-3-319-58443-0](https://doi.org/10.1007/978-3-319-58443-0)
- [22]. C. Curtis, *Fuel* 37 (1992) 46–54. DOI: [10.2307/25305520](https://doi.org/10.2307/25305520)
- [23]. T.W. Kennedy, F.L. Roberts, K.W. Lee, *Transportation Research Record* 968 (1984) 45–54.
- [24]. C. Oliviero Rossi, P. Caputo, N. Baldino, F.R. Lupi, D. Miriello, R. Angelico, *Int. J. Adhes. Adhes.* 70 (2016) 297–303. DOI: [10.1016/j.ijadhadh.2016.07.013](https://doi.org/10.1016/j.ijadhadh.2016.07.013)
- [25]. C. Oliviero Rossi, P. Caputo, N. Baldino, E. Ildyko Szerbc, B. Teltayev, *Int. J. Adhes. Adhes.* 72 (2017) 117–122. DOI: [10.1016/j.ijadhadh.2016.10.015](https://doi.org/10.1016/j.ijadhadh.2016.10.015)
- [26]. H. Ollendorf, D. Schneider, *Surf. Coat. Technol.* 113 (1999) 86–102. DOI: [10.1016/S0257-8972\(98\)00827-5](https://doi.org/10.1016/S0257-8972(98)00827-5)
- [27]. J. Grenfell, N. Ahmad, Y. Liu, A. Apeagyei, D. Large, G. Airey, *Road Mater. Pavement Design* 15 (2014) 131–152. DOI: [10.1080/14680629.2013.863162](https://doi.org/10.1080/14680629.2013.863162)
- [28]. S. Cui, B.R.K. Blackman, A.J. Kinloch, A.C. Taylor, *Int. J. Adhes. Adhes.* 54 (2014) 100–111. DOI: [10.1016/j.ijadhadh.2014.05.009](https://doi.org/10.1016/j.ijadhadh.2014.05.009)
- [29]. C. Oliviero Rossi, B. Teltayev, R. Angelico, *Appl. Sci.* 7 (2017) 524. DOI: [10.3390/app7050524](https://doi.org/10.3390/app7050524)
- [30]. Z. Liu, X. Huang, A. Sha, H. Wang, J. Chen, C. Li, *Materials* 12 (2019) 605. DOI: [10.3390/ma12040605](https://doi.org/10.3390/ma12040605)
- [31]. C. Oliviero Rossi, P. Caputo, G. De Luca, L. Maiuolo, S. Eskandarsefat, C. Sangiorgi, *Appl. Sci.* 8 (2018) 229. DOI: [10.3390/app8020229](https://doi.org/10.3390/app8020229)
- [32]. D.D. Eberl, V.A. Drits, J. Srodon, *Am. J. Sci.* 298 (1998) 499–533. DOI: [10.2475/ajs.298.6.499](https://doi.org/10.2475/ajs.298.6.499)
- [33]. J. Drelich, J.D. Miller, R.J. Good, *J. Colloid Interf. Sci.* 179 (1996) 37–50. DOI: [10.1006/jcis.1996.0186](https://doi.org/10.1006/jcis.1996.0186)
- [34]. K. Seo, M. Kim, J.K. Ahn, D.H. Kim, *Korean J. Chem. Eng.* 32 (2015) 2394–2399. DOI: [10.1007/s11814-015-0034-x](https://doi.org/10.1007/s11814-015-0034-x)
- [35]. J. Drelich, *J. Adhesion* 63 (1997) 31–51. DOI: [10.1080/00218469708015212](https://doi.org/10.1080/00218469708015212)
- [36]. P. Caputo, D. Miriello, A. Bloise, N. Baldino, O. Mileti and G.A. Ranieri, *Int. J. Adhes. Adhes.* 102 (2020) 102680. DOI: [10.1016/j.ijadhadh.2020.102680](https://doi.org/10.1016/j.ijadhadh.2020.102680)
- [37]. M. Nazirizad, A. Kavussi, A. Abdi, *Constr. Build. Mater.* 84 (2015) 348–353. DOI: [10.1016/j.conbuildmat.2015.03.024](https://doi.org/10.1016/j.conbuildmat.2015.03.024)
- [38]. R.A. Young, in: R.A. Young (Ed.), *The Rietveld Method*, Oxford University Press, 1993, pp. 1–38.
- [39]. A.F. Gualtieri, G.D. Gatta, R. Arletti, G. Artioli, P. Ballirano, G. Cruciani, A. Guagliardi, D. Malferrari, N. Masciocchi, P. Scardi, *Periodico di Mineralogia* 88 (2019) 147–151.
- [40]. P. Caputo, V. Loise, A. Crispini, C. Sangiorgi, F. Scarpelli, C. Oliviero Rossi, *Colloid. Surface. A* 571 (2019) 50–54. DOI: [10.1016/j.colsurfa.2019.03.059](https://doi.org/10.1016/j.colsurfa.2019.03.059)
- [41]. C. Klein and C.S. Hurlbut, J.D. Dana. The 22nd edition of the manual of mineral science: (after James D. Dana), New York : J. Wiley, 2002.
- [42]. K.V. Cashman, B.D. Marsh, *Contr. Mineral. Petrol.* 99 (1988) 292–305. DOI: [10.1007/BF00375363](https://doi.org/10.1007/BF00375363)
- [43]. W.A. Deer, R.A. Howie, J. Zussman, J.F.W. Bowles, D.J. Vaughan, *Rock-Forming Minerals, Volume 5A: Non-Silicates: Oxides, Hydroxides and Sulphides*, 2011.